

# Heterogeneous Dynamics and Pressure Dependence of the Dynamics in van der Waals Liquids

Samy Merabia<sup>\*,‡</sup> and Didier Long<sup>\*,†,§</sup>

Laboratoire de Physique des Solides, CNRS and Université de Paris XI, Bat. 510, 91405 Orsay Cédex, France, and Departament de Física Fonamental, Universitat de Barcelona, Martí i Franqués 1, 08028 Barcelona, Spain

Received November 13, 2007; Revised Manuscript Received February 27, 2008

**ABSTRACT:** We consider the dependence of the dynamics in nonpolar liquids as a function of pressure close to the glass transition. We show how dynamical heterogeneities lead naturally to a dependence of the dominant relaxation time  $\tau_\alpha$  on two independent parameters, i.e., on both pressure  $P$  and temperature  $T$  or on both density  $\rho_{eq}$  and temperature, without assuming the presence of energy barriers. The predictions of our model regarding the dependence of  $\tau_\alpha$  as a function of pressure are discussed and compared to experimental data. Our model can account quantitatively for this dependence in the case of nonpolar molecular liquids such as 1,1'-di(4-methoxy-5-methylphenyl)cyclohexane (BMMPC) and 1,1'-bis(*p*-methoxyphenyl)cyclohexane (BMPC) up to pressures a few hundred atmospheres and can account approximately for the slope  $[d \log(\tau_\alpha)]/dP$  at zero pressure in the case of flexible polymers such as poly(methyltolylsiloxane) (PMTS) and poly(methylphenylsiloxane) (PMPS). We propose that nonpolar molecular liquids could be more systematically studied as model systems for understanding in detail glass transition mechanisms, which should be helpful for making progress on more complex systems, e.g., polymers with both polar and nonpolar interactions.

## 1. Introduction

When cooling a glass-forming liquid, one observes a rapid increase of the viscosity.<sup>1,2</sup> Usually,  $T_g$  is arbitrarily defined as the temperature at which the viscosity reaches  $10^{12}$  Pa·s in simple liquids or at which the dominant relaxation time  $\tau_\alpha$  becomes larger than about  $\tau_g \sim 10^2$  s. Typically, the viscosity or the dominant relaxation time increases by 12 orders of magnitude between  $T_g + 100$  K and  $T_g$ , and their evolution over this temperature range is described by the Vogel–Fulcher–Tammann (VFT) law (or William–Landel–Ferry (WLF) law in the context of polymer).<sup>3</sup> The aim of this paper is to consider quantitatively the dependence of the dynamics in van der Waals liquids as a function both on the temperature and the density or, equivalently, as a function of the temperature and pressure in the WLF range and in particular above but close to  $T_g$ . This issue has been the topic of much experimental work for several decades and is still under intense debate.<sup>4–26</sup> When considering the dependence of the dynamics as a function of both the average density and of the temperature, the dependence on the latter has often been attributed to the presence of energy barriers. In particular, by comparing the respective contribution of each of these macroscopic parameters, Tarjus et al. concluded that, as a universal rule, the relevant parameter for controlling the dynamics is the temperature, the role of the density being secondary.<sup>27,28</sup> However, Roland and co-workers<sup>19,20,29,30</sup> have argued that the liquids considered by these authors belong to a specific class of liquids, i.e., polar liquids able to build strong intermolecular bonds. On the contrary, by considering nonpolar molecular liquids such as 1,1'-di(4-methoxy-5-methylphenyl)cyclohexane (BMMPC) and 1,1'-bis(*p*-methoxyphenyl)cyclohexane (BMPC), or nonpolar polymeric liquids such as poly(methyltolylsiloxane) (PMTS) and poly(methylphenylsiloxane) (PMPS), Roland and co-workers<sup>19,20,29,30</sup> concluded that the role

of density is prevalent for nonpolar liquids. We argue in this paper that, in the case of nonpolar liquids, and especially in the case of nonpolar molecular liquids, *the temperature and pressure dependence can be explained quantitatively by taking into account density fluctuations.*

In particular, we argue in this paper that dynamical heterogeneities play a crucial role for a quantitative description of the dynamics as a function of both pressure and temperature. Indeed, another important feature of the glass transition is the heterogeneous nature of the dynamics close to  $T_g$ , which has been demonstrated over the past 15 years.<sup>31–37</sup> These studies have demonstrated the coexistence of domains with relaxation time distributions spread over more than 4 decades at temperatures typically 20 K above  $T_g$ . The characteristic size  $\xi$  of these domains, estimated by NMR,<sup>31</sup> is typically 3–4 nm in the case of van der Waals liquids. For dealing with the dependence of the dynamics as a function of both temperature and pressure, we use a model proposed in refs 38–41 which aimed at accounting for dynamical heterogeneities in nonpolar liquids. Several other theoretical approaches regarding the dynamics of supercooled liquids have been proposed over the past decade. The mode coupling model (see e.g. ref 42) deals with hydrodynamic-like equations for the density fluctuations and involves a nonlinear coupling with the density. This model predicts an arrest of the dynamics at a temperature  $T_{mc}$  above  $T_g$  and breaks down at molecular time scales of order  $10^{-9}$  s. It appears thus to be useful only at temperatures more than 80 K above the glass transition, as a consequence of its perturbative approach.<sup>43</sup> Note however that this temperature ( $T_g + 80$  K) is indicative and depends in general on the considered polymer.<sup>1</sup> Numerical simulations are also used for studying liquids dynamics. For instance, some evidence that the dynamics is heterogeneous have been given using this technique.<sup>44</sup> However, molecular dynamics simulations cannot be used for studying dynamics on time scales longer than  $10^{-6}$  s or for studying equilibrium dynamics at temperatures below  $T_g + 80$  K. Other models aimed at describing spin dynamics have been proposed (see e.g. ref 45). However, the connection with real liquids dynamics has not been established yet. Other approaches

\* To whom correspondence should be addressed. E-mail: didier.long-exterieur@eu.rhodia.com.

<sup>†</sup> CNRS and Université de Paris XI.

<sup>‡</sup> Universitat de Barcelona.

<sup>§</sup> Present address: CNRS/Rhodia, Rhodia Recherches et Technologies, 85 rue des freres Perret, F-69192 Saint Fons cedex, France.

for dealing with the glass transition deserve to be mentioned, such as the energy landscape description.<sup>46</sup> On the other hand, the connection between barriers distribution and density in these various models is not explicit.

An essential point regarding our model is that the dynamics we consider is a function of the whole spectrum of density fluctuations on scale  $\xi$ . At equilibrium, the latter is a function of both the average density  $\rho_{eq}$  and of the temperature or of both the temperature and the pressure. Thus, intrinsically, the equilibrium dynamics predicted by our model is a function of both the temperature and the average density without assuming the presence of specific energy barriers. We deal with van der Waals liquids, i.e., nonpolar liquids, with only van der Waals attractions. Paradigms of such liquids include molecular liquids such as BMMPC and BMPC where hydrogen bonds are absent. In the case of polymeric liquids, we assume that chain flexibility is temperature independent. It means that our model aimed at describing the behavior of flexible polymer chains for which activated motions along the backbone are irrelevant. We compare then in detail the prediction of our model with experimental data regarding two nonpolar molecular liquids (BMPC and BMMPC) which have been studied recently by Paluch et al.<sup>20</sup> We will show that our model can account quantitatively for their relaxation dynamics as a function of pressure, up to a few hundred atmospheres, for a wide range of temperatures. We will also consider the case of flexible silicone polymers (PMTS and PMPS) and show that our model can account approximately for the slope  $[d \log(\tau_\alpha)]/dP$ , also recently studied by Paluch et al.<sup>19</sup> We will also discuss the case of poly(vinyl acetate) (PVAc). This polymer has relatively weak polar interactions (see e.g. ref 47). This allows to illustrate the limitations of the present development of this model when activated motions along the backbone or weak hydrogen bonds are present in the liquid. Note however that we will see that our model can account approximately for the slope  $[d \log(\tau_\alpha)]/dP$  at atmospheric pressure in this case also.

In ref 41, we have shown that dynamical heterogeneities are at the heart of specific features of aging and rejuvenating dynamics in van der Waals liquids.<sup>48,49</sup> The mechanism that we proposed for rejuvenating dynamics is the following. First, when heating a sample, the system starts to populate faster and faster subunits (on scale  $\xi$ ), but for a while, the densest subunits have not relaxed. Then, the latter dissolve in the more mobile environment by diffusion process of the denser subunits in the faster ones. We propose here that closely related relaxation mechanisms can account quantitatively for the dependence of the dynamics of van der Waals liquids as a function of both pressure and temperature.

The paper is organized as follows. In section IIA we describe the thermodynamics of van der Waals liquids as a function of the temperature and the pressure by extending our previous model.<sup>38</sup> It allows in particular for a quantitative description of the evolution of density as a function both on pressure and on temperature. In section IIB, we introduce notations and definitions regarding the WLF law. Then we discuss and precise some aspects of the model for the glass transition in the bulk that we proposed in refs 38–41 (section IIC). In section III, we discuss briefly how the results regarding the dependence of  $\tau_\alpha$  as a function of  $T$  and  $P$  are presented in the literature. In section IV, we extend our model for the glass transition and derive its prediction regarding the evolution of  $\tau_\alpha$  as a function of pressure. We discuss our results in section V.

## II. Model for the Glass Transition in van der Waals Liquids

**A. Density of van der Waals Liquids as a Function of Both Temperature and Pressure.** We extend here the thermodynamical model for van der Waals liquids proposed in ref 38. The latter was devised in the absence of an applied pressure. We consider here the equilibrium at a given temperature  $T$  and applied pressure  $P$ . The free energy per degree of freedom can be written as

$$F(\rho) = F_0(\rho) + \frac{P}{\rho} = -\Phi C \rho^2 - T \ln(\rho_0 - \rho) + \frac{P}{\rho} \quad (1)$$

where  $F_0$  is the free energy per degree of freedom:<sup>38</sup>

$$F_0 = U - TS = -\Phi C \rho^2 - T \ln(\rho_0 - \rho) \quad (2)$$

The quantity

$$U = -\Phi C \rho^2 \quad (3)$$

is the attractive energy per degree of freedom due to van der Waals forces exerted by the other monomers and

$$S = \ln(\rho_0 - \rho) \quad (4)$$

is the entropy per degree of freedom.  $\Phi$  is a constant of about 4, and  $C$  is the Hamaker constant of the liquid.<sup>50</sup>  $\rho$  is the density of degrees of freedom (number of particles per unit volume), and  $\rho_0$  is a close-packing density of the degrees of freedom, also expressed in number per unit volume. It is the density of degrees of freedom of the liquid extrapolated when the temperature goes to zero under zero applied pressure (or under the negligible atmospheric pressure). For a detailed discussion about this definition see ref 38, section 2.  $T$  is the thermal energy expressed in joules. At room temperature, the order of magnitude is  $4 \times 10^{-21}$  J. The density at equilibrium is given by minimizing the free energy (1):

$$\left(\frac{\partial F}{\partial \rho}\right)_{T,P} = 0 \quad (5)$$

with the condition that the equilibrium is metastable:

$$\left(\frac{\partial^2 F}{\partial \rho^2}\right)_{T,P} > 0 \quad (6)$$

At zero pressure, we found in ref 38 that there is one solution to this pair of equations when the temperature  $T$  is lower than a temperature  $T_c$  with

$$T_c = \frac{\Phi C}{2} \rho_0^2 \quad (7)$$

The temperature  $T_c$  is the only energy scale of the model and depends on the strength of the van der Waals attraction between monomers (or molecules for a simple liquid). The relevant temperature regime for the model presented here is  $T \ll T_c$ , which is well satisfied, since for usual polymers or molecular liquids  $T_c$  is found to be of order 1000 K.<sup>38,39</sup> Room temperature corresponds then to a low-temperature regime, for which the density fluctuations correlation length is comparable to the monomer length.

The presence of an applied pressure increases the temperature  $T_c$ . Thus, the relevant regime corresponds still to the case where  $T \ll T_c$ . The equilibrium density  $\rho = \rho_{eq}(T, P)$  satisfies thus the equation

$$\rho^4 - \rho_0 \rho^3 + \frac{T}{4T_c} \rho_0^2 \rho^2 + \frac{\rho_0^2 P}{4T_c} \rho - \frac{\rho_0^3 P}{4T_c} = 0 \quad (8)$$

This equation is best solved numerically by the Laguerre method.<sup>51</sup> Among the four solutions to eq 8, only one corresponds to the physical solution and satisfies

$$\rho < \rho_0 \quad (9)$$

One can define the free volume fraction by

$$\epsilon = \rho \left( \frac{1}{\rho} - \frac{1}{\rho_0} \right) \quad (10)$$

Actually, it was argued in ref 38 that the eqs 1, 5, and 6 are mean-field equations that do not take fully the incompressibility of the monomers into account. The latter constraint leads to an increase of the free volume as calculated in the mean-field approximation and an increase of the bulk modulus. The free volume  $\epsilon$  is then increased to give

$$\epsilon' = (1 + \beta)\epsilon \quad (11)$$

where  $\beta$  is a positive number of order unity. The density is then changed into

$$\frac{1}{\rho'} = \frac{1}{\rho_0} + (1 + \beta) \left( \frac{1}{\rho} - \frac{1}{\rho_0} \right) \quad (12)$$

where  $\rho$  is the solution of the eq 5. The bulk modulus is given by

$$K = \left( \frac{1}{\rho} \left( \frac{\partial \rho}{\partial P} \right)_T \right)^{-1} \quad (13)$$

Alternatively, one might write the equivalent definition:

$$K = \rho^3 \left( \frac{\partial^2 F}{\partial \rho^2} \right)_T = \rho^3 \left( \frac{\partial^2 F_0}{\partial \rho^2} \right)_T + 2P \quad (14)$$

At zero pressure, one can solve this equation exactly to obtain

$$K_0 = \frac{T\rho_0}{2} \left( 1 + \left( 1 - \frac{T}{T_c} \right)^{1/2} \right)^3 \left( \frac{1}{(1 - (1 - T/T_c)^{1/2})^2} - \frac{T_c}{T} \right) \quad (15)$$

As we discussed in ref 38, the bulk modulus calculated according to eq 6 is found to be smaller than the experimental value  $K_{\text{exp}}$ :

$$K_0 < K_{\text{exp}} \quad (16)$$

The reason is the same as previously discussed: the mean-field equations do not take fully into account the incompressible nature of the monomers. Doing this led to a rescaling of the bulk modulus by a factor we denoted  $1/\gamma^2$  in ref 38. One has then

$$K = \frac{1}{\gamma^2} K_0 = K_{\text{exp}} = T \frac{n}{2} \left( 1 + \left( 1 - \frac{T}{T_c} \right)^{1/2} \right)^3 \times \left( \frac{1}{(1 - (1 - T/T_c)^{1/2})^2} - \frac{T_c}{T} \right) \quad (17)$$

where we have defined  $n$  by

$$n \equiv \frac{\rho_0}{\gamma^2} \quad (18)$$

The numbers  $\gamma$  and  $\beta$  are adjustable parameters of order unity.  $n$  is an effective number of degrees of freedom per unit volume at close packing (it is expressed in  $\text{m}^{-3}$ ) and is typically of order a few  $10^{27} \text{ m}^{-3}$ . However, these quantities are measurable experimentally as we will discuss below.

Now that the microscopic description of the thermodynamical model has been proposed, we work only with macroscopic quantities. Therefore, from now on,  $\rho$  denotes the density expressed in  $\text{g cm}^{-3}$  of the systems, and  $\rho_0$  denotes the density extrapolated at  $T = 0 \text{ K}$  expressed also in  $\text{g cm}^{-3}$ . The latter are directly measurable quantities. The parameters  $\beta$  and  $\rho_0$  can be measured by fitting the dependence of density as a function of temperature (see Figures 3–6 in ref 38). Similarly, the equilibrium density is given by eq 8, and the free volume has

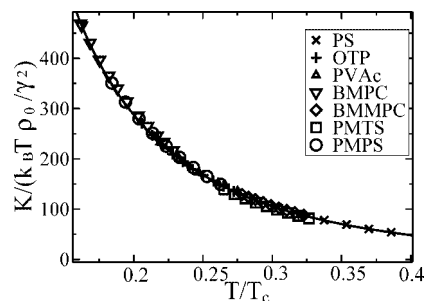


**Figure 1.** Master curve for the bulk moduli of PS, PVAc, OTP, BMPC, BMMPC, PMTS, and PMPS as a function of the reduced temperature  $T/T_c$ .

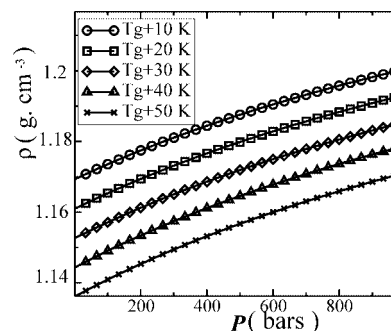


**Figure 2.** Density of PVAc as a function of pressure. The data (symbols) are from ref 17; the continuous curve is given by our model. The corresponding parameters are given in Table 1. The different curves correspond to different temperatures:  $\circ$ ,  $T_g + 10 \text{ K}$ ;  $\square$ ,  $T_g + 20 \text{ K}$ ;  $\diamond$ ,  $T_g + 30 \text{ K}$ ;  $\triangle$ ,  $T_g + 40 \text{ K}$ ;  $\times$ ,  $T_g + 50 \text{ K}$ .

to be rescaled according to eq 12. Let us denote by  $\rho'(T, P)$  the density solution of these equations. The dependence of the density as a function of pressure is thus given by

$$\rho_{\text{eq}}(T, P) = \rho'(T, \gamma^2 P) \quad (19)$$

The rescaling of the pressure dependence of the density in eq 19 ensures that the relation 13 is satisfied. As already mentioned, the parameters  $n$  and  $T_c$  are determined for each polymer by fitting the data regarding the bulk modulus, as a function of temperature, with eq 17. We plotted in Figure 1 the evolution of the bulk modulus at atmospheric pressure for various liquids as a function of temperature. These liquids are *o*-terphenyl (OTP), poly(vinyl acetate) (PVAc), 1,1'-di(4-methoxy-5-methylphenyl)cyclohexane (BMMPC), 1,1'-bis(*p*-methoxyphenyl)cyclohexane (BMPC), poly(methyltolylsiloxane) (PMTS), and poly(methylphenylsiloxane) (PMPS). The data regarding PVAc and OTP are drawn from refs 52 and 53, those regarding BMPC and BMMPC are from ref 20, and those regarding PMTS and PMPS are from ref 19. The parameter  $1/\gamma^2$  can be measured by fitting the evolution of density as a function of pressure (see eq 19), which we did by plotting in Figures 2 and 3 the evolution of the density of PVAc and BMPC as a function of pressure up to 100 MPa, for various temperatures. Note that the pressure dependence of OTP, PMMA, PS, BMPC, PMTS, PMPS, polyisobutylene (PIB), and poly(*n*-butyl methacrylate) (PBMA) can be fitted up to 100 MPa as well as those shown here. The parameters  $n$ ,  $\rho_0$ ,  $\beta$ , and  $1/\gamma^2$  for OTP, PVAc, BMMPC, BMPC, PMTS, and PMPS are given in Table 1. The values of the corresponding parameters for PIB, PBMA, PS, and poly(methyl methacrylate) (PMMA) are given in ref 38. We conclude here that our model allows for a quantitative description of the evolution of  $\rho_{\text{eq}}(P, T)$  for van der Waals liquids over a wide range of temperature and pressure.

**B. WLF Law.** Here we introduce notations which allow us to write the standard WLF law in a form that we can use more



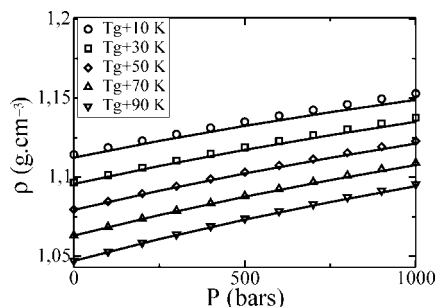


**Figure 3.** Equilibrium density of BMPC as a function of pressure. Solid lines correspond to density calculated by solving eq 8 and by taking the monomer incompressibility constraint into account. The symbols are experimental data taken from ref 20.

readily later in the text. Throughout the paper,  $\tau_\alpha$  denotes the time which dominates the mechanical behavior of the liquid or melt. The variation of this relaxation time or of the viscosity in the bulk is given by the empirical WLF law (or VFT law in the context of simple liquids):<sup>3,54</sup>

$$\log\left(\frac{\tau_\alpha}{\tau_\alpha(T_0)}\right) = \frac{-C_1(T - T_0)}{C_2 + T - T_0} \quad (20)$$

where  $T_0$  is a temperature of reference, not to be confused with the Vogel temperature  $T_\infty = T_0 - C_2$ , which is sometimes also denoted by  $T_0$ . Here, typically,  $T_0$  is close to the glass transition temperature  $T_g$ , and  $\tau_\alpha(T_0)$ , the relaxation time at temperature  $T_0$ , is a macroscopic time scale, e.g., comparable to 100 s.  $C_1$  and  $C_2$  are constants which depend on the considered polymers. One can see that the relaxation time is supposed to diverge at  $T_\infty$ . Typically, one has  $T_\infty \sim T_g - 50$  K. Note however that in practice, at temperatures below  $T_g - 30$  K, the relaxation times are too long to be measurable, which means that eq 20 is in general checked only at temperatures above  $T_g - 20$  K or more. Note however that these temperatures are indicative and depend in general on the considered polymer.<sup>1</sup> It was shown in ref 39 that eq 20 may be expressed in the equivalent form

$$\tau_\alpha(T) = \tau_0 \exp\left(\frac{\Theta}{\tilde{\epsilon}(T)}\right) \quad (21)$$

which depends explicitly on the density and is more readily useful for our glass transition model.  $\Theta$  is a number of order unity, and  $\tau_0$  is a ballistic time between collisions typically of order  $10^{-13}$  s. The quantity

$$\tilde{\epsilon} = \frac{\tilde{\rho}_0 - \rho_{\text{eq}}}{\rho_0} \quad (22)$$

is the “dynamical” free volume fraction. In the free volume picture, the quantity  $\Theta/\tilde{\epsilon}$  is interpreted as the number of molecules which must be pushed for allowing a jump of a given molecule. The density  $\tilde{\rho}_0$  is smaller than  $\rho_0$ , a fact which has been noted many years ago<sup>54</sup> and for which we have no interpretation at this point. This fact is equivalent to the fact that the temperature at which the relaxation time diverges according to the WLF law,  $T_\infty$ , is finite. Note that the difference between  $\tilde{\rho}_0$  and  $\rho_0$  is very significant. For instance, in PS at the glass transition ( $T_g = 375$  K), one finds  $\epsilon \approx 0.2$ , while  $\tilde{\epsilon} \approx 0.02$ . The corresponding parameters for PVAc, BMPC, BMMPC, PMTS, and PMPS are given in the Table 2. The corresponding data are drawn from refs 55 and 56 in the case of PVAc, ref 20 in the case of BMPC and BMMPC, and ref 19 for PMTS and PMPS.

**C. Model for the Glass Transition in the Bulk.** As mentioned in the Introduction, it has been shown that the dynamics close to the glass transition are heterogeneous, with the coexistence between relatively fast subunits and relatively

slow ones. In the model described in refs 38–40, we proposed that slow subunits correspond to upward density fluctuations and fast subunits to downward density fluctuations on a particular scale of  $N_c = \rho V$ . On a given scale, density fluctuations follow the Boltzmann law

$$P(\delta\rho) \sim \exp(-\delta\rho^2 KV/2\rho_{\text{eq}}^2 T) \quad (23)$$

By using the results of our thermodynamical model for van der Waals liquids, it is useful to define

$$\frac{\delta\rho}{\rho} = \frac{(\alpha - \alpha_\eta)\epsilon}{\sqrt{N_c}} \quad (24)$$

$\alpha$  is a dimensionless quantity, which characterizes the amplitude of the considered fluctuations, and follows therefore the Gaussian statistics. The bare internal relaxation time of subunits corresponding to fluctuations  $\alpha$  is then

$$\tau(\alpha) = \tau_0 \exp\left(\frac{\Theta}{\tilde{\epsilon} - (\alpha - \alpha_\eta)\epsilon/N_c^{1/2}}\right) \quad (25)$$

$$P(\alpha) = \frac{1}{(2\pi)^{1/2}} \exp\left(-\frac{\alpha^2}{2}\right)$$

Note that  $\alpha_\eta$  is defined by

$$\int_{\alpha_\eta}^{\infty} P(\alpha) d\alpha = p_c \quad (26)$$

where  $p_c$  is a 3D percolation threshold, typically close to 0.1.<sup>40</sup> The dominant relaxation time for the viscosity of the liquid is  $\tau_\alpha = \tau(\alpha_\eta)$  as given by eq 25. The number  $\alpha_\eta \sim 1$  is such that dimensionless density fluctuations larger than  $\alpha_\eta$  (corresponding to relaxation times larger than  $\tau_\alpha$ ) percolate (see Figure 4). Thus, in a mechanical experiment, one probes  $\tau_\alpha$ , while a wide distribution of relaxation times coexist in the system.<sup>38–40</sup> These fluctuations have to be considered on a scale  $N_c$  of order a few hundred of monomers. In ref 39 we proposed an expression for the scale  $N_c$  by considering two competing relaxation mechanisms: (1) the individual monomer jump time, which tends to increase sharply in subunits with large density fluctuations, and (2) the relaxation of density fluctuations, which is a collective process on the considered scale. We discuss the determination of  $N_c$  now.

*a. Scale of Dynamical Heterogeneities.* For calculating the value of  $N_c$ , the issue is to determine which processes lead to the longest dominant relaxation time in a supercooled liquid. We are primarily concerned here by relaxation processes which control the viscosity of the system. As described above, the longest relaxation times will take place in subunits with large density fluctuations. The WLF law corresponds to the relaxation time of these slow subunits. It means that  $\tilde{\rho}_0$  takes the large density fluctuations into account. Therefore, the monomer jump time

$$\tau_j = \tau_0 \exp\left(\frac{\Theta}{\tilde{\epsilon}}\right) = \tau_\alpha \quad (27)$$

corresponds to monomers in dense subunits ( $\alpha = \alpha_\eta$ ). On scale  $N$ , typical free volume fluctuations are of order  $\alpha\epsilon/N^{1/2}$ , where  $\alpha$  is a number of order 1. Therefore, monomers with jump time given by eq 27 coexist with monomers with jump time given by

$$\tau_j^\pm = \tau_0 \exp\left(\frac{\Theta}{\tilde{\epsilon} + \alpha^\pm \epsilon/N^{1/2}}\right) \quad (28)$$

which can be either much smaller ( $\tau_j^-$ , with  $\alpha^\pm = \alpha^+ > 0$ ) or much larger ( $\tau_j^+$ , with  $\alpha^\pm = \alpha^- < 0$ ) than  $\tau_\alpha$ . Equation 28 means that by considering small scales one can find monomers with very large monomer jump time ( $\alpha^\pm \sim -1$ ) as given by the free volume model, with probability of order 1. The time  $\tau_j^+$  would

**Table 1. Parameters for the Thermodynamics of PVAc, OTP, BMPC, BMMPC, PMTS, and PMPS**

liquid	$T_g$ (K)	$n$ ( $10^{27} \text{ m}^{-3}$ )	$1/\gamma^2$	$T_c$ (K)	$\rho_0$ ( $\text{g cm}^{-3}$ )	$\beta$	molar mass (g)	ref
PVAc	310	2.9	2.12	1430	1.469	3.01	NC	52
OTP	241	1.98	3.2	1359	1.33	2.8	81	53
BMPC	232	1.57	2.5	1463	1.345	3.43	296	20
BMMPC	261	4.3	2.05	1078	1.285	1.35	322	20
PMTS	258	3.	2.13	1143	1.508	1.85	147	19
PMPS	243	1.6	0.83	1591	1.314	2.44	134	19

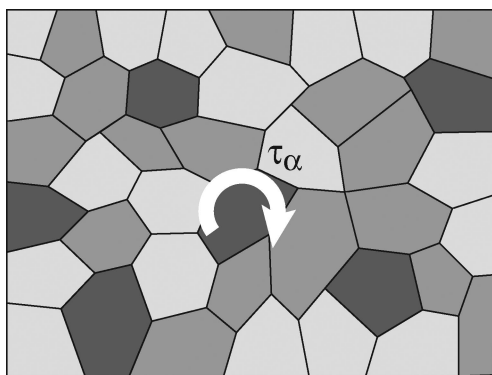
**Table 2. WLF Parameters of PVAc, BMPC, BMMPC, PMTS, and PMPS**

liquid	$C_1$	$C_2$ (K)	$T_0$ (K)	$T_g$ (K)	$\theta = \Theta/2.3$	$\tilde{\rho}_0$ ( $\text{g cm}^{-3}$ )	$\log \tau(T_0)/\tau_0$	ref
PVAc	15.57	60.0	311.1	310.0	0.536	1.2311	15.57	55, 56
BMPC	19.34	80.24	238	232	0.668	1.175	17.0	20
BMMPC	16.9	80.2	269	261	0.519	1.145	15.0	20
PMTS	15.09	43.99	263	258	0.360	1.307	15.0	19
PMPS	15.54	46.44	242	243	0.310	1.177	15.0	19

be the monomer jump time if the density was maintained fixed by imaginary walls. On the other hand, the density of the subunit has a finite lifetime. For  $\tau_j^+$  to be the effective monomer jump time, the environment of the monomer, i.e., the density of the subunit, has to be kept at a large density during a time interval of at least  $\tau_j^+$ . Thus, the lifetime of the considered density fluctuation has to be at least  $\tau_j^+$ .

Let us now consider the lifetime  $\tau_{\text{life}}$  of density fluctuations on the scale of  $N$  monomers. The corresponding length scale is  $\xi = aN^{1/3}$ , where  $a$  is one monomer length. We consider positive density fluctuations with large bare monomer jump time. Such a subunit is surrounded by other subunits corresponding to various density fluctuations, some of them corresponding to lower density fluctuations. Then, the dense subunits we consider will dissolve in the surrounding subunits of lower density and faster dynamics by a diffusion process. This is what we schematize in Figure 5. This Figure represents a zoom of Figure 4. In the latter, we represent only the subunits but do not represent the molecules (or the monomers) within. In Figure 5 we look within the subunits for describing their internal relaxation processes.

This diffusion process occurs at the boundary of the considered subunit, and the monomer time jump is that of the lower density neighboring subunits in which it diffuses. Since the lifetime of density fluctuations is controlled by a diffusion process, this lifetime is proportional to the scale  $\xi^2 \propto N^{2/3}$  that we consider. Indeed, we assume that density fluctuations on scale  $q^{-1}$  relax with the usual diffusion laws, i.e.,  $\tau(q) \propto q^{-2} \tau_{\text{fast}}$ , where  $\tau_{\text{fast}}$  is the local monomer time jump in the rapid neighboring subunit as given by eq 28 with  $\alpha^\pm \sim 1$  (see in



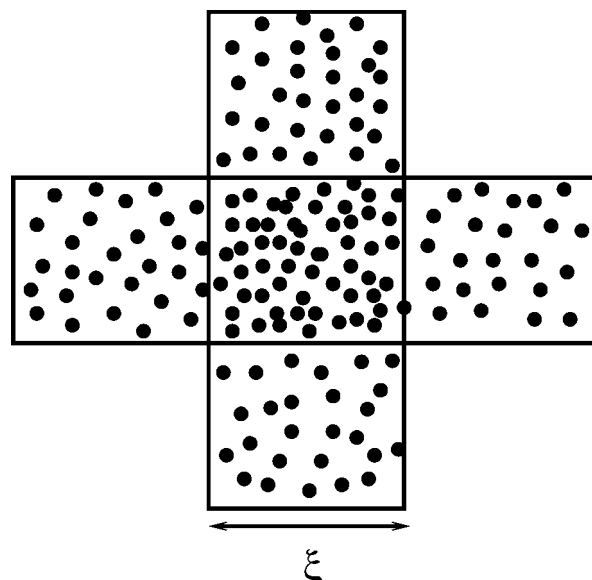
**Figure 4.** Final relaxation mechanism in a van der Waals liquid, in the WLF (or VFT) regime. Dynamical subunits have been divided in three types: fast subunits (light gray), subunits of internal relaxation time  $\tau_\alpha$  (gray), and subunits with internal relaxation time  $\tau \gg \tau_\alpha$  (dark gray). The ensemble of subunits with internal relaxation time larger or equal to  $\tau_\alpha$  percolate. The dominant relaxation time is  $\tau_\alpha$  since the slowest subunits can rotate or diffuse in those with dominant time  $\tau_\alpha$ .

Figure 5). Therefore, the lifetime of a considered density fluctuation on the scale  $N$  is then

$$\tau_{\text{life}} \sim \tau_0 N^{2/3} \exp\left(\frac{\Theta}{\tilde{\epsilon} + \alpha \epsilon / N^{1/2}}\right) \quad (29)$$

where  $\alpha$  is of order 1, since the diffusion will take place primarily through the most rapid environment with non-negligible probability. Then, the larger the scale, the longer the lifetime of density fluctuations.

In summary here, we deduce from the preceding discussions that by considering small enough scales one can find, with probability of order one, very dense subunits. The relaxation time of these subunits should be therefore very long (given by eq 28 with  $\alpha < 0$ ). However, another relaxation process competes with the individual monomer jumps and corresponds to the relaxation of density fluctuations. At small scale, this process is faster than the individual monomer jump time one would observe if the density was maintained fixed. At small scale it is therefore the dominant relaxation time (see Figure



**Figure 5.** Two mechanisms compete for determining the  $\alpha$ -relaxation: (1) local reorganization of free volume at fixed local density and (2) diffusion of the densest subunit in the more mobile neighboring subunits. A dense subunit can be melted by its mobile neighbors. A subunit of large density will melt and relax in a longer time if it is surrounded only by subunits that are themselves relatively slow. The lifetime of a dense subunit surrounded by much faster subunits with internal relaxation time  $\tau_{\text{fast}}$  is  $\tau_{\text{life}} = \tau_{\text{fast}} N^{2/3}$ . This time is frequently shorter than the relaxation time a dense subunit would have if its overall density was maintained fixed by imaginary walls. The latter would be  $\tau_j^+$  as given in the text by eq 28 with  $\alpha < 0$ .

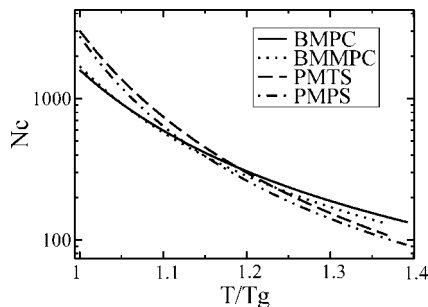


**Figure 6.** Dominant scale of dynamical heterogeneities for BMPC, BMMPC, PMTS, and PMPS as a function of temperature, at atmospheric pressure. This scale is derived from our model, with as adjustable parameters only those of the WLF law of the corresponding liquid.

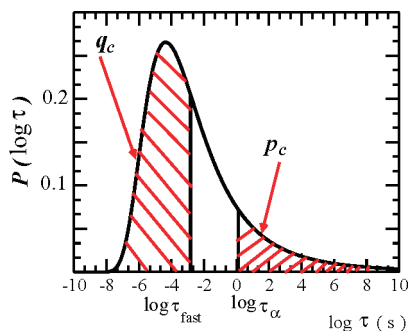


**Figure 7.** Equilibrium relaxation time distribution at temperature  $T_g$ .  $\tau_\alpha$  is the relaxation time of dense subunits that percolate (fraction  $p_c$ ) while  $\tau_{\text{fast}}$  is the typical relaxation time of mobile units (fraction  $q_c$ ). At equilibrium, one has  $\tau_\alpha = \tau_{\text{fast}} N_c^{2/3}$ .

5). Therefore, the largest relaxation times in the system are determined by the relation

$$\tau_{\text{life}} = \tau_j^+ \quad (30)$$

which yields

$$N_c \approx \frac{\Theta^2 \epsilon^2}{\epsilon^4} \frac{1}{\left( \ln \left( \frac{\Theta^2 \epsilon^2}{\epsilon^4} \right) \right)^2} \quad (31)$$

The scale  $\xi = a N_c^{1/3}$  ( $a$  is one monomer length) is thereby the smallest scale at which the density fluctuations lifetime is equal or larger than  $\tau_\alpha$ . Density fluctuations on smaller scales are irrelevant being too short-lived. In Figure 6 we plotted the evolution of  $N_c$  with temperature for BMPC, BMMPC, PMTS, and PMPS. The main feature of the scale  $N_c$  is that it is of order a few hundred typically close to  $T_g$  and that it decreases when increasing the temperature.<sup>39</sup>

*b. Distribution of Relaxation Times.* We represented in Figure 7 the distribution of relaxation times when the sample is at equilibrium. By definition then, one has the relation

$$\tau_\alpha = N_c^{2/3} \tau_{\text{fast}} \quad (32)$$

where the time  $\tau_{\text{fast}}$  is the local relaxation time of fast neighboring subunits and corresponds to the  $q_c$  fastest subunits:

$$\int_0^{\tau_{\text{fast}}} P(\tau) d\tau = q_c \quad (33)$$

where  $P(\tau)$  is here the equilibrium distribution of relaxation times. Equivalently, the relaxation time  $\tau_{\text{fast}}$  can be expressed as

$$\tau_{\text{fast}} = \tau_0 \exp \left( \frac{\Theta}{\tilde{\epsilon} + (\alpha_c + \alpha_\eta) \epsilon / N_c^{1/2}} \right) \quad (34)$$

where  $\alpha_c$  is a positive coefficient related to the fraction  $q_c$ :

$$\int_{-\infty}^{-\alpha_c} \frac{1}{(2\pi)^{1/2}} \exp \left( -\frac{\alpha^2}{2} \right) = q_c \quad (35)$$

$q_c$  is to be determined. The respective values of  $p_c$  and  $q_c$  are not arbitrary. In refs 38 and 40 we have shown that the value of the 3D percolation threshold,  $p_c$ , can be chosen as approximately equal to 10%. We did this by considering the dynamics in thin films and their thickness dependence, which allowed to determine the bulk percolation threshold  $p_c$ . In ref 41 we proposed that  $q_c = 30\%$  so as we could obtain the right rejuvenating dynamics for various polymeric liquids. Thus, for the sake of consistency, we keep these respective values for the parameters  $p_c$  and  $q_c$ .

### III. Relaxation Time as a Function of Density and Temperature

We consider now the dynamics in a van der Waals supercooled liquid as a function of both temperature and pressure or, equivalently, as a function of both temperature and density. Many experiments have shown that the dynamics in liquids is a function of both variables.<sup>5–16,18–26</sup> Several ways for quantifying the relative importance of the variables ( $T, P$ ), or ( $T, \rho$ ) are used in the literature. For the sake of clarity and for making easier the comparison between various presentations of the results, we list them below.

**A. Isochrone Coefficients.** In order to compare the respective role of temperature and pressure, Alba-Simionesco et al.<sup>27,28</sup> have defined an isochrone expansion coefficient  $\alpha_\tau = -\beta_\tau$  with

$$\beta_\tau = \frac{1}{\rho} \left( \frac{\partial \rho}{\partial T} \right)_\tau = \frac{1}{\rho} \frac{\left( \frac{-\partial \log \tau_\alpha}{\partial T} \right)_\rho}{\left( \frac{\partial \log \tau_\alpha}{\partial \rho} \right)_T} > 0 \quad (36)$$

If the dynamics depended only on the average density, the coefficient  $\alpha_\tau$  should be identically zero. By writing

$$\left( \frac{\partial \log \tau_\alpha}{\partial T} \right)_\rho = \left( \frac{\partial \log \tau_\alpha}{\partial T} \right)_\rho + \left( \frac{\partial \log \tau_\alpha}{\partial \rho} \right)_T \left( \frac{\partial \rho}{\partial T} \right)_\rho \quad (37)$$

or equivalently

$$\left( \frac{\partial \log \tau_\alpha}{\partial T} \right)_\rho = -\rho \left( \frac{\partial \log \tau_\alpha}{\partial \rho} \right)_T (\beta_\tau + \beta_\rho) \quad (38)$$

where we have used the usual thermal expansion coefficient

$$\beta_\rho = -\frac{1}{\rho} \left( \frac{\partial \rho}{\partial T} \right)_P = \frac{\chi_T}{T} \quad (39)$$

one sees that the ratio  $\beta_\tau/\beta_\rho$  is a measure of the respective contribution of the temperature and of the density on the evolution of  $\tau_\alpha(T, \rho)$ .

**B. Free Energy Barriers at Constant Volume or Pressure.** It is also customary to introduce the following quantities, which are analogous to free energy barriers at constant volume or at constant pressure, respectively:

$$E_V = R \left( \frac{\partial \log \tau_\alpha}{\partial T^{-1}} \right)_V \quad (40)$$

$$E_P = R \left( \frac{\partial \log \tau_\alpha}{\partial T^{-1}} \right)_P \quad (41)$$

With the preceding definitions it is straightforward to show the relations

$$E_P = E_V + RT\rho\chi_T\left(\frac{\partial \log \tau_\alpha}{\partial \rho}\right)_T \quad (42)$$

Therefore, the ratio between  $E_V$  and  $E_P$  reads

$$\frac{E_V}{E_P} = 1 - \frac{\beta_P}{\beta_P + \beta_\tau} \quad (43)$$

This ratio is comprised between 0 and 1. The value of this ratio is also a measure of the relative importance of the temperature and of the pressure regarding the dynamics.

**C. Master Curve.** Let us note also that it has been observed for several liquids that the dependence of the dominant relaxation time as a function of the temperature and the volume for instance can be put on a master curve, function of the variable  $T^{-1}V^{-\kappa}$  only:

$$\ln(\tau_\alpha(T, V)) = \ln \tilde{\tau}(T^{-1}V^{-\kappa}) \quad (44)$$

When this relation holds, it is straightforward to deduce the following result:

$$\frac{E_V}{E_P} = \frac{1}{1 + \kappa\chi_T} \quad (45)$$

The parameter  $\kappa$  is also a measure of the relative importance of the temperature and the density for controlling the dynamics.

**D. Experimental Measurements of  $\tau_\alpha$  as a Function of Pressure.** In many experiments, the quantity which is directly measured is the variation of the dominant relaxation time as a function of the pressure at fixed temperature. In this paper, we will consider the prediction of our model regarding the evolution of  $\tau_\alpha$  as a function of pressure. To make comparisons with discussions proposed in the literature, it is therefore useful to relate the latter to other quantities mentioned above. The derivative of  $\tau_\alpha$  according to the pressure, at fixed temperature, can be written as

$$\left(\frac{\partial \log \tau_\alpha}{\partial P}\right)_T = \left(\frac{\partial \log \tau_\alpha}{\partial \rho}\right)_T \left(\frac{\partial \rho}{\partial P}\right)_T = \frac{\rho}{K} \left(\frac{\partial \log \tau_\alpha}{\partial \rho}\right)_T \quad (46)$$

from which we obtain

$$K \left(\frac{\partial \log \tau_\alpha}{\partial P}\right)_T = \frac{\left(-\frac{\partial \log \tau_\alpha}{\partial T}\right)_P}{\beta_\tau + \beta_P} \quad (47)$$

or

$$1 + \frac{\beta_\tau}{\beta_P} = \frac{-T \left(\frac{\partial \log \tau_\alpha}{\partial T}\right)_P}{\chi_T K \left(\frac{\partial \log \tau_\alpha}{\partial P}\right)_T} \quad (48)$$

In the last relation, the numerator on the right-hand side is given by the WLF law. The dimensionless thermal expansion and the bulk modulus at the denominator are known quantities. Thus, this last relation relates directly the derivative of the dominant relaxation time according to the pressure at fixed temperature to the coefficient  $\beta_\tau$ .

**E. Discussion.** All parameters or ratio defined above are used to assess the relative importance of the temperature and pressure and/or density on the dynamics. For instance, regarding isochrone coefficients (A), the temperature is usually considered a more important macroscopic parameter than the density when  $\beta_P \lesssim \beta_\tau$ .<sup>20,27,28,57</sup> Regarding the so-called free-energy barriers at constant volume or pressure (B), the temperature is considered a more important parameter than the density whenever the ratio  $E_V/E_P$  is larger than 0.5.<sup>18–20,29,58,59</sup> Regarding the master curve methodology (C), taking into account the fact that typically  $\chi_T$

$\sim 0.2$ , the temperature is generally considered a more important parameter than the density when  $\kappa$  is smaller than about 4 or 5.<sup>30,60–64</sup> Finally, when measuring independently the evolution of  $\tau_\alpha$  as a function of temperature, at fixed pressure, and as a function of pressure, at fixed temperature, one considers in general that the temperature is a more important parameter than the density if the term on the right-hand side of eq 48 is smaller than 2. All these definitions are explicitly equivalent on the expressions presented above.

However, though these quantities are useful to assess the relative importance of pressure and temperature, or of temperature and density on the dynamics, they can do it only as far as temperature and density are considered as macroscopic parameters. For instance, the terminology of energy barriers for defining  $E_V$  (eq 40) is misleading, since a nonzero value does not necessarily mean that energy barriers are present in the systems as we will see below. More generally, a quantitative interpretation of the microscopic relaxation mechanisms based on these various quantities is not straightforward. In particular, we will see below that taking free volume fluctuations into account allows for a quantitative explanation of  $E_V/E_P$  ratios up to values approximately equal to 0.5 or, equivalently, values of  $1 + \beta_\tau/\beta_P$  up to approximately 2 without introducing energy barriers in the model.

#### IV. Model for the Dependence of $\tau_\alpha$ on Both Temperature and Pressure

We aim now at quantifying the prediction of our model regarding the dependence of the dominant relaxation time  $\tau_\alpha$  as a function of both the temperature and pressure. To this end we consider first the evolution of the dominant relaxation time  $\tau_\alpha$  as a function of temperature, at fixed equilibrium density. The following discussion helps to illustrate the mechanisms which are relevant in the general case. Let us consider a sample at various temperatures whereas the density is maintained fixed by applying a pressure. Consider a sample at equilibrium at temperature  $T$  under the applied pressure  $P$ . The distribution of density fluctuations on scale  $N_c$  is given by

$$P(\rho) \sim \exp\left(-\frac{KV}{2T} \left(\frac{\rho - \rho_{eq}(T, P)}{\rho_{eq}(T, P)}\right)^2\right) \quad (49)$$

where  $\rho_{eq}(T, P)$  is the average equilibrium density and  $V = N_c/\rho_{eq}(T, P)$  is the volume of subunits with  $N_c$  monomers. In particular, the width of the distribution is

$$\sigma = \sqrt{\frac{T}{KV}} \quad (50)$$

Let us suppose that we start from an equilibrium situation under atmospheric pressure. Then, let us increase the temperature at constant average density by applying a pressure  $P$ . At fixed density, the distribution of density fluctuations widens according to eq 50. The reasons are the following: (1) The bulk modulus is a decreasing function of temperature. (2) The scale  $N_c$  and thus  $V$  is a decreasing function of temperature. Both effects tend to decrease the denominator in eq 50. (3) The numerator in eq 50 increases because it is the temperature itself. On heating, less dense subunits are thus created, as one can see in Figure 8. The distribution of internal relaxation times of subunits widens. According to the discussion regarding the determination of the scale of dynamical heterogeneities, the dominant relaxation time  $\tau_\alpha$  is given by

$$\tau_\alpha = N_c^{2/3} \tau_{fast} \quad (51)$$

where the right-hand side of eq 51 corresponds to the lifetime of the 10% or so densest fluctuations. Since the relaxation time  $\tau_{fast}$  of less dense subunits decreases,  $\tau_\alpha$  decreases also.



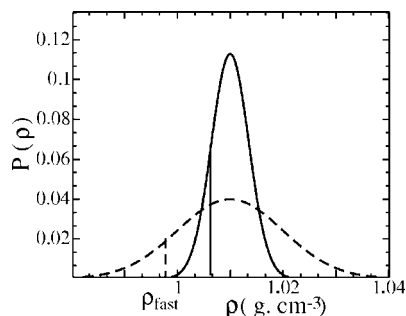


**Figure 8.** Density fluctuations distributions at fixed average density, for two different temperatures:  $T_g$  and  $T_g + 50$  K. At high temperature, the distribution widens because the bulk modulus is smaller.

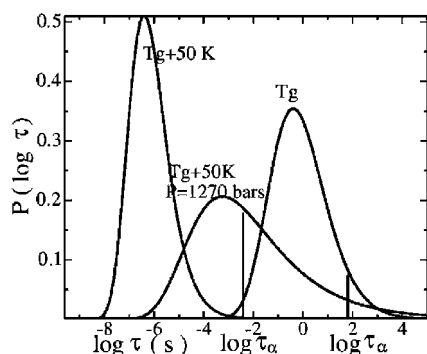


**Figure 9.** Distribution of relaxation times at a constant value of the average/equilibrium density, as derived from our model. We plotted the relaxation time distribution of PVAc at  $T_g$  under atmospheric pressure. The density is then  $1.177 \text{ g cm}^{-3}$ . We plotted also the distribution of relaxation time at equilibrium at  $T_g + 50$  K, still for an average/equilibrium density of  $1.177 \text{ g cm}^{-3}$  (the applied pressure is then 1270 bar), also the relaxation time distribution at  $T_g + 50$  K under atmospheric pressure. We see that by increasing the temperature, at fixed density, the distribution of relaxation times is broader: fast subunits are created and melt the denser subunits in a shorter time that at the same density but lower temperature: the dominant relaxation time  $\tau_\alpha$  decreases.

Therefore, we have shown that even at constant average density, the dominant relaxation time decreases when increasing the temperature. This mechanism is also at the origin of the temporal asymmetry between aging dynamics and rejuvenating dynamics as discussed in ref 41.

To illustrate how the dynamics can be changed by increasing the temperature at fixed average density, consider the following example. In Figure 9 we plotted the distribution of relaxation times at equilibrium at temperature  $T_g$  under atmospheric pressure. The average equilibrium density takes the value  $1.177 \text{ g cm}^{-3}$ . We plotted also the relaxation time distribution at temperature  $T_g + 50$  K under an applied pressure  $P = 1270$  atm, a pressure such that the average density is maintained fixed. We see that at higher temperatures the density fluctuation distribution widens. One obtains thus subunits of lower density than at  $T_g$ , which are more rapid. As discussed before, on heating the liquid, less denser subunits having fast internal relaxation times are created and correspondingly the relaxation time distribution widens toward faster relaxation times. As a consequence, the dominant relaxation time  $\tau_\alpha$  diminishes due to the presence of faster subunits in the liquid (eq 51). For instance, the dominant relaxation time is 4 decades smaller in these conditions that at  $T_g$  under atmospheric pressure (see Figure 9).

What the preceding discussion shows is that the WLF parameters change with an applied pressure. Indeed, the WLF law is an empirical law which gives the evolution of the

dominant relaxation time as a function of temperature or can be generalized as an empirical law giving this dependence as a function of both temperature and pressure. The value of the parameters of this law are not predicted by any theory. They assume values which allow to fit experimental data. Their values take into account all the relevant relaxation mechanisms. The latter remain of course incompletely known or understood. What the discussion above shows is that e.g. increasing the temperature at fixed density accelerates relaxation mechanisms, by the same mechanisms that explain the temporal asymmetry between cooling and melting of a glassy polymer.<sup>41</sup> The less dense subunits relax according to their free volume while the denser subunits relax with a diffusion process involving mobile neighboring subunits. Thus, applying a pressure  $\delta P$  changes  $\tilde{\rho}_0(P)$  or  $\tilde{\epsilon}(P)$  in such a way that the equality (51) remains satisfied. The dominant relaxation time  $\tau_\alpha$  in an equilibrium situation, at temperature  $T$  and pressure  $P$ , is given by

$$\tau_\alpha(P) = \tau_0 \exp\left(\frac{\Theta}{\tilde{\epsilon}(P)}\right) \quad (52)$$

where

$$\tilde{\epsilon}(P) = \frac{\tilde{\rho}_0(P) - \rho_{eq}(P)}{\rho_0} \quad (53)$$

is the analogous of the eq 22 where we assume that  $\tilde{\rho}_0$  is a function of pressure, and where  $\rho_{eq}(P)$  is the mean (and equilibrium) value of the density under the applied pressure  $P$  at the considered temperature. We show, in the Appendix, that the dominant relaxation time  $\tau_\alpha$  increases with the pressure according to

$$\frac{d}{dP}(\ln \tau_\alpha) = \frac{d}{dP}\left(\frac{\Theta}{\tilde{\epsilon}}\right) = \frac{\partial}{\partial \rho_{eq}}\left[\frac{\Theta}{\tilde{\epsilon} + (\alpha_c + \alpha_\eta)\epsilon/N_c^{1/2}(P)}\right] \frac{d}{dP}[\rho_{eq}(P)] \quad (54)$$

where  $\alpha_c$  is related to the fraction  $q_c$  through eq 35. Note that the first term in brackets on the right-hand side of eq 54 corresponds to the logarithm of the relaxation time of fast subunits  $\tau_{fast}$  (see eq 34). The quantity  $\epsilon(\alpha_c + \alpha_\eta)/N_c^{1/2}$  in the denominator of the right-hand side of eq 54 is a dimensionless measure of the difference between the densest and less dense subunits. The evolution of  $N_c$  with the applied pressure is given by

$$N_c(P) = \frac{\Theta^2 \epsilon^2(P)}{\tilde{\epsilon}^4(P)} \frac{1}{\left(\ln\left(\frac{\Theta^2 \epsilon^2(P)}{\tilde{\epsilon}^4(P)}\right)\right)^2} \quad (55)$$

which is obtained in a similar way as the temperature dependence of  $N_c$  (eq 31) and with

$$\epsilon(P) = \frac{\rho_0 - \rho_{eq}(P)}{\rho_0} \quad (56)$$

which generalizes eq 10. There is no additional adjustable parameter in eq 54 as we had in previous discussions. The value of  $q_c$  is chosen to be 30% as it was chosen when considering the rejuvenating dynamics of van der Waals liquids in ref 41, and  $\alpha_\eta$  assumes the value corresponding to  $p_c = 0.1$  to be consistent with thin film  $T_g$  shifts.<sup>40</sup> As we shall see below, eq 54 does not allow for a completely exact description of the evolution of  $\tau_\alpha$  as a function of pressure for all liquids. To compare various systems we will consider the following equation:



$$\frac{d}{dP}(\ln \tau_\alpha) = \frac{d}{dP} \left( \frac{\Theta}{\tilde{\epsilon}} \right) = \frac{\partial}{\partial \rho_{\text{eq}}} \left[ \frac{\Theta}{\tilde{\epsilon} + \zeta(\alpha_c + \alpha_\eta)\epsilon/N_c^{1/2}(P)} \right] \frac{d}{dP}[\rho_{\text{eq}}(P)] \quad (57)$$

which is the same as eq 54 apart from the factor  $\zeta$  in front of the term  $\alpha_c + \alpha_\eta$  on the right-hand side of the equation. The exact evolution equation corresponds to the value  $\zeta = 1$ , which will be solved. We will also solve our model with different values of  $\zeta$  and compare the results. Note in particular that the term  $(\alpha_c + \alpha_\eta)\epsilon(P)/N_c^{1/2}(P)$  in eq 54 is not an adjustable parameter here. Their exact value is set for obtaining the right rejuvenating dynamics ( $\alpha_c$ , see ref 41); the right dynamical behavior in thin films ( $\alpha_\eta$ , see ref 40); the right width of relaxation time distribution ( $N_c$ , see ref 39). As we will see below, the parameter  $\zeta$  accounts thus for some details or aspects not taken into account by our model. Among the latter, there are the possibility of activated motion along the backbone of polymers or the presence of, relatively weak hydrogen bonds (PVAc). Another aspect is that we assume that density fluctuations are Gaussian. This may not be entirely true on the considered scale, and the value of  $\zeta$  might describe thus some distance to pure Gaussian fluctuations. In particular, non-Gaussianity of density fluctuations is likely to depend on pressure.

## V. Results and Discussion

We consider the prediction of our model and the comparisons with experimental data. We consider two paradigms of van der Waals molecular liquids, BMPC and BMMPC. Then, we analyze the case of two nonpolar flexible polymers, PMTS and PMPS, and discuss also the case of PVAc which is a polymer with relatively weak polar interactions. First, we discuss the slope of  $\log(\tau_\alpha(T, P))$  at atmospheric pressure.

**A. Slope of  $\log(\tau_\alpha(T, P))$  at Atmospheric Pressure.** In Table 3 we wrote the values of the slope at zero pressure  $[d \log \tau_\alpha(P = 0)]/dP$  for BMPC, BMMPC, PMTS, PMPS, and PVAc, at various temperatures. We compare them with the values predicted by our model, without additional adjustable parameters

**Table 3.  $[d \log \tau_\alpha(P = 0)]/dP$  for BMPC, BMMPC, PMTS, PMPS, and PVAc at Various Temperatures<sup>a</sup>**

liquid	temp (K)	(d log $\tau_\alpha$ )/dP expt	(d log $\tau_\alpha$ )/dP theor value	(d log $\tau_\alpha$ )/ dP theory with $\zeta \neq 1$
BMPC	254		7.9	6.5
	269	5.8	5.4	5.5
	279	5.2	4.4	3.9
BMMPC	278.95	6.8	7.8	6.4
	288.85	6.0	6.1	5.2
	295.35	5.8	5.5	4.5
	307.55	5.0	4.2	3.6
PMPS	253	9.8	13.1	9.5
	263	7.5	9.1	6.2
	273	6.0	6.0	4.1
	293		3.5	2.6
	313		2.3	1.8
PMTS	276.6	8.2	12.0	6.4
	283	6.2	9.4	5.8
	293	4.7	6.7	4.5
	303		5.1	3.5
	313		4.0	2.8
PVAc	333	5.2	6.7	
	353	3.2	4.4	
	373	2.5	3.2	
	393	1.9	2.4	
	413	1.4	1.9	

<sup>a</sup> Comparisons between the results of our model and experimental data.<sup>19,20</sup> The quantity  $[d \log \tau_\alpha(P = 0)]/dP$  is expressed in units of  $10^{-3} \text{ bar}^{-1}$ .

**Table 4. Ratio  $1 + \beta_T/\beta_P$ , with the Slope  $[d \log \tau_\alpha(P = 0)]/dP$  Estimated at Atmospheric Pressure, for the Same Liquids and Temperatures as in Table 3<sup>a</sup>**

liquid	temp (K)	$1 + \beta_T/\beta_P$ expt	$1 + \beta_T/\beta_P$ theory	$1 + \beta_T/\beta_P$ theory with $\zeta \neq 1$
BMPC	254		1.25	1.52
	269	1.26	1.36	1.35
	279	1.21	1.42	1.60
BMMPC	278.95	1.53	1.33	1.6
	288.85	1.42	1.39	1.6
	295.35	1.33	1.39	1.7
	307.55	1.26	1.51	1.76
PMPS	253	1.6	1.18	1.62
	263	1.57	1.33	1.8
	273	1.44	1.45	2.12
	293		1.68	2.27
	313		1.87	2.39
PMTS	276.6	1.82	1.25	2.32
	283	1.91	1.28	2.10
	293	2.0	1.40	2.08
	303		1.47	2.14
	313		1.55	2.21
PVAc	333	1.35	1.04	
	353	1.53	1.10	
	373	1.48	1.15	
	393	1.54	1.23	
	413	1.75	1.28	

<sup>a</sup> Comparisons between the results of our model and experimental data.<sup>19,20</sup> The quantity  $[d \log \tau_\alpha(P = 0)]/dP$  is expressed in  $\text{bar}^{-1}$ .

as compared to the WLF law of the considered liquids (i.e.,  $\zeta = 1$ ). We see that the slope predicted by our model is close to experimental data in the case of the molecular liquids BMPC and BMMPC and quite close for the larger temperatures in the case of PMTS, PMPS, and PVAc. In Table 4 we sum up the experimental values of the ratio  $1 + \beta_T/\beta_P$ , with the slope  $[d \log \tau_\alpha(P = 0)]/dP$  estimated at atmospheric pressure, for the same liquids and temperatures as in Table 3.

Note that all the considered values for  $1 + \beta_T/\beta_P$  are smaller than 2, which, according to some frequent definitions in the literature, means that the dominant macroscopic parameter for these liquids is the density rather than temperature. At this point, one must question the significance or relevance of such definitions. Indeed, according to the description of relaxation processes that we proposed here, we show that we cannot infer directly the role of density fluctuations from the influence of the macroscopic parameter which is the average density. Increasing the temperature results in an increase of density fluctuations, which leads to an acceleration of the dynamics. Attributing the effect to the temperature or to the density—through the fluctuations of the latter—is just a matter of definition. What must be noted here is that such values of the ratio  $1 + \beta_T/\beta_P$  can be explained by the role of density fluctuations. A more relevant issue is: can we infer from macroscopic measurements such as those regarding  $\beta_T$  and  $\beta_P$  the presence of specific energy barriers, such as hydrogen bonds between different molecules, or activated motion along the backbone which might contribute to the final  $\alpha$ -relaxation? For instance, polymers are not freely jointed chains. The Kuhn length of polymers depends on temperature. On the other hand, reducing the Kuhn length contributes to accelerate the  $\alpha$ -process. Such an effect is not taken into account in the model presented here. Discrepancies between our results and experimental data might be therefore an indication of the presence of such mechanisms. For instance, our model cannot—and is not intended for—describe relaxation processes in liquids such as glycerol for which  $\alpha$ -relaxation is overwhelmingly determined by hydrogen bonds.<sup>27</sup> For such liquids, the ratio  $\beta_T/\beta_P$  can be larger than 10 or even 20. On the other hand, when the effect of specific energy barriers are small or nonexistent, the evolution of the dominant relaxation time is expected to be given by our model, and one expects  $1 + \beta_T/\beta_P$

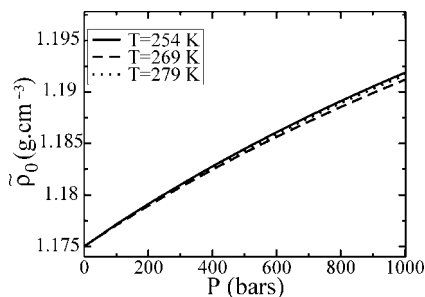


Figure 10. Evolution of  $\tilde{\rho}_0$  as a function of pressure for BMPC.

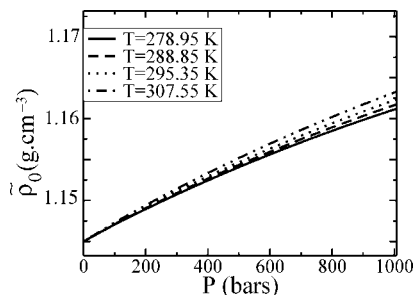


Figure 11. Evolution of  $\tilde{\rho}_0$  as a function of pressure for BMMPC.

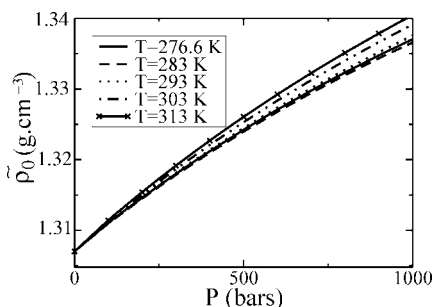


Figure 12. Evolution of  $\tilde{\rho}_0$  as a function of pressure for PMTS.

$\lesssim 2$ . Our conclusion here is also consistent with the one by Roland and co-workers.<sup>19,20</sup> In refs 29 and 30, Roland and co-workers compared the ratio  $\beta_T/\beta_P$  of various liquids. Most of these ratios were comprised between 0.5 and 2, and they concluded that density and temperature play a similar role regarding the dynamics. According to the model presented here, these values for  $\beta_T/\beta_P$  and thus the respective effect of the pressure and temperature can be accounted for by density fluctuations. Our conclusion is that large  $\beta_T/\beta_P$  ratio, such as those observed by Tarjus and co-workers,<sup>27,28</sup> are typical of H-bonded liquids, which behave differently than nonpolar liquids. On the contrary, we conclude that for nonpolar liquids the dynamics is the result of steric or compaction effects and that the glass transition is the result of congestion due to a lack of free volume.

**B. Evolution of  $\tau_\alpha$  as a Function of Pressure.** To further test our model, we considered the evolution of  $\tau_\alpha(T, P)$  as a function of pressure. The evolution of  $\tilde{\epsilon}(P)$  as a function of pressure is obtained by solving the differential equation (54). The evolutions of  $\tilde{\rho}_0(P)$  for BMPC, BMMPC, PMTS, and PMPS as a function of pressure are plotted in Figures 10, 11, 12, and 13, respectively. In Figure 14 we plotted the evolution of  $N_c$  as a function of pressure, for various temperatures. The main feature here is about a 5-fold increase between atmospheric pressure and 100 MPa. In Figures 15, 16, 17, and 18, we plotted the dominant relaxation time of BMPC, BMMPC, PMTS, and PMPS, respectively, for several temperatures above the glass transition temperature at atmospheric pressure. The logarithm

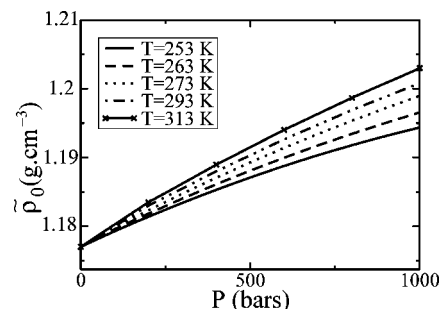


Figure 13. Evolution of  $\tilde{\rho}_0$  as a function of pressure for PMPS.

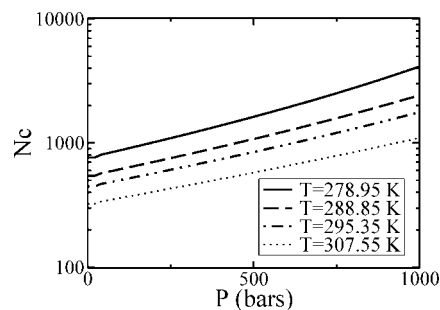


Figure 14. Evolution of  $N_c$  as a function of pressure for BMMPC, at four different temperatures larger than  $T_g = 261$  K.

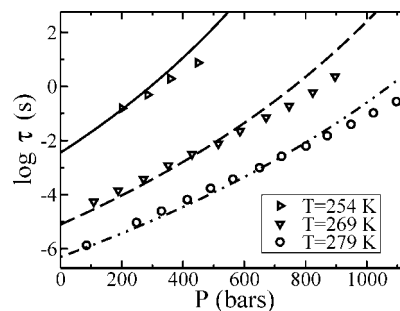


Figure 15. Dominant relaxation time  $\tau_\alpha$  of BMPC as a function of pressure. The results for three temperatures above the glass transition temperature at  $P = 0$  are displayed. The curves are the results from our model (eq 54) while the symbols are experimental taken from ref 20.

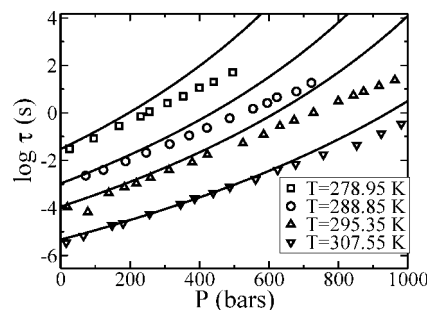
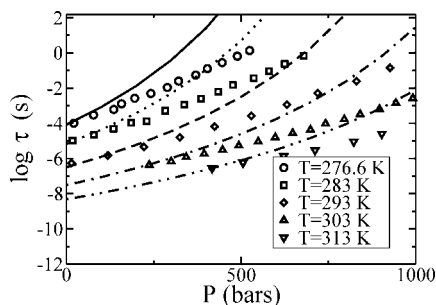
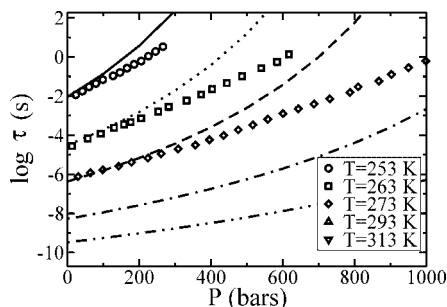


Figure 16. Dominant relaxation time  $\tau_\alpha$  of BMMPC as a function of pressure. The results for four temperatures above the glass transition temperature at  $P = 0$  are displayed. The curves are the results from our model (eq 54). The symbols are data extract from ref 20.

of  $\tau_\alpha$  increases roughly linearly with pressure, with a slope that increases when the temperature is lowered. On all these curves, the low-pressure behavior of the results obtained from our model is close to the experimental data. For higher temperatures, this low-pressure regime extends up to a few tens of MPa. For the lower values of the temperature, our model essentially predicts the right value for the slope at atmospheric pressure. What can



**Figure 17.** Dominant relaxation time  $\tau_\alpha$  of PMTS as a function of pressure. The results for five temperatures above the glass transition temperature at  $P = 0$  are displayed. The curves are the results from our model (eq 54). The data are from ref 19.



**Figure 18.** Dominant relaxation time  $\tau_\alpha$  of PMPS as a function of pressure. The results for three temperatures above the glass transition temperature at  $P = 0$  are displayed. The curves are the results from our model (eq 54). The data are from ref 19.

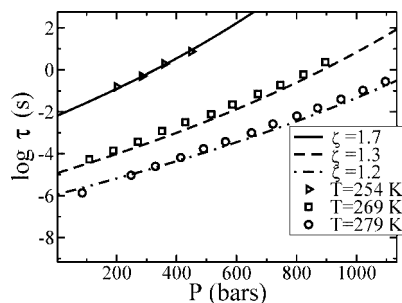


**Figure 19.** Dominant relaxation time  $\tau_\alpha$  of BMPC as a function of pressure. The results for three temperatures above the glass transition temperature at  $P = 0$  are displayed. The curves are the results from our model (eq 57 with the appropriate prefactor  $\zeta$  indicated). The data are from ref 20.

be noted also is that our theoretical results are in better agreement with experimental data in the case of the molecular liquids BMPC and BMMPC than in the case of the silicone polymers PMTS and PMPS.

To make more quantitative comparisons, we had to introduce various values of the parameter  $\zeta$  (eq 57), which can be considered as a measure of the uncompleteness of our model. The results are given in Figures 19, 20, 21, and 22. We see that it is possible to reproduce the experimental results up to 100 MPa with values of  $\zeta$  of order 1. The larger the temperature, the closer to one the value of the parameter  $\zeta$ . Note that at temperatures  $T \approx T_g + 35$  K the values of  $\zeta$  for BMPC, BMMPC, PMTS, and PMPS are 1.2, 1.3, 1.8, and 1.7, respectively. We see thus that our model is very close of predicting the right behavior of the molecular liquids BMPC and BMMPC and quite close for the silicone polymers PMTS and PMPS. The evolution of the dominant relaxation time as a function of pressure for PVAc is plotted in Figure 23 for various temperatures. The theoretical curves are obtained by solving

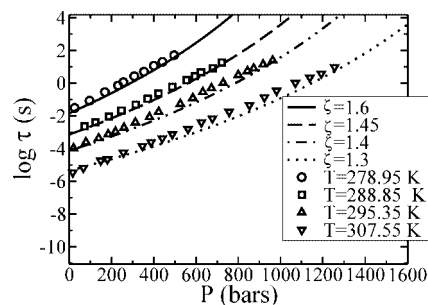


**Figure 20.** Dominant relaxation time  $\tau_\alpha$  of BMMPC calculated by using eq 57 with the appropriate prefactor  $\zeta$ , as a function of pressure, for various temperatures. For the considered pressures, one sees that the logarithm of the dominant relaxation time increases linearly with the pressure. The slope is about 4 decades/kbar at  $T = 307.55$  K  $\approx T_g + 47$  K. The experimental data (symbols) are from ref 20.

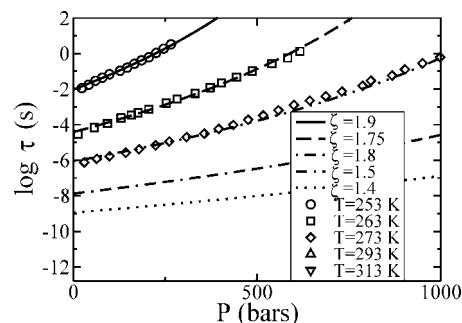


**Figure 21.** Dominant relaxation time  $\tau_\alpha$  of PMPS as a function of pressure. The results for five temperatures above the glass transition temperature at  $P = 0$  are displayed. The curves are the results from our model (eq 57 with the appropriate prefactor  $\zeta$  indicated). The data are from ref 19.

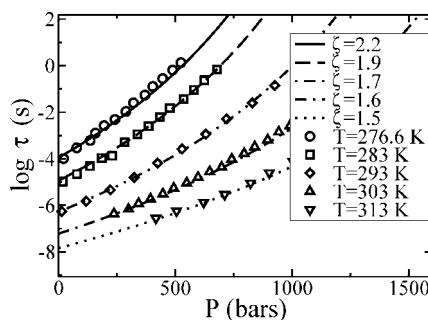


**Figure 22.** Dominant relaxation time  $\tau_\alpha$  of PMTS calculated by using eq 51 with the appropriate prefactor in eq 57 indicated, as a function of pressure, for various temperatures. For the considered pressures, the logarithm of the dominant relaxation time increases linearly with the pressure. The slope is about 5 decades/kbar at  $T = 279$  K  $\approx T_g + 37$  K. The symbols are experimental data extract from ref 19.

the differential equation (54). We can see that the slope at  $P = 0$  is quite good, whereas the subsequent evolution at larger pressures is not so good.

**C. Discussion.** Our results show that our model is close to explain quantitatively the evolution of the dominant relaxation time as a function of pressure, over a wide temperature range, in the case of nonpolar liquids. Indeed, we could calculate slopes at zero pressure of the pressure dependence of the dominant relaxation time  $\tau_\alpha$ , which are close to experimental data, especially at relatively large temperatures and in the case of BMPC and BMMPC (see Table 3). We did this without introducing new parameters as compared to the WLF law at atmospheric pressure for BMPC, BMMPC, PMTS, PMPS, and PVAc. Regarding the evolution of  $\tau_\alpha$  as a function of pressure,

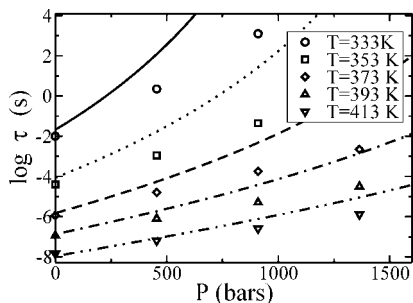


**Figure 23.** Dominant relaxation time  $\tau_\alpha$  of PVAc calculated by using eqs 51 and 54, as a function of pressure, for various temperatures. For the considered pressures, the logarithm of the dominant relaxation time increases linearly with the pressure. The slope is about 5 decades/kbar at  $T = 279 \text{ K} \approx T_g + 37 \text{ K}$ . Symbols are data taken from ref 18.

we could obtain quantitative results by a small modifications of our equations (parameter  $\zeta$ ), especially in the case of BMPC and BMMPC, for pressure up to 1 kbar.

The fact that our model allows for explaining almost quantitatively the pressure dependence of BMPC and BMMPC shows that nonpolar molecular liquids should be considered as model systems for making progress in the understanding of glass transition mechanisms, thereby paving the way for a more precise understanding of more complex systems. The relatively small discrepancy between the results of our model and experimental data regarding PMPS and PMTS might be the result of thermally activated motion along the chain (flexibility) or also regarding pending groups ( $\beta$ -relaxation) that should be taken into account in further theoretical developments. In addition to the reasons mentioned in the case of PMTS and PMPS, the discrepancy between the results of our model and experimental data in the case of PVAc might be due to the presence of hydrogen bonds. The corresponding enthalpy, about 4 kcal/mol (see e.g. ref 47), is smaller than 5–10 times the thermal energy  $T$ , whereas the barrier for  $\alpha$ -relaxation close to  $T_g$  is of order  $30T$ . The contribution of hydrogen bonds, though relatively small, is not negligible and should be taken into account also in further extensions of this model.

## VI. Conclusion

We have shown how to account for the dependence of the dominant relaxation time as a function of both temperature and the pressure in van der Waals liquids. We have shown that taking into account density fluctuations allows for almost quantitatively describing the dependence of the dynamics as a function of pressure for nonpolar molecular liquids and nonpolar flexible polymers. Paradigms of the former are BMPC and BMMPC whereas PMTS and PMPS are typical examples of nonpolar flexible polymeric liquids. In the case of PVAc, which displays weak polar interactions, our model was also close to account quantitatively for the initial slope  $d \log(\tau_\alpha)/dP$  of the pressure dependence of the dynamics. The description of the  $\alpha$ -process that we proposed in refs 38 and 39 is at the heart of the corresponding dynamics. The mechanism that we propose for that is the following. First, when heating a sample at constant density, the systems populate faster subunits because of the broadening of the density fluctuations. This process results in a shortening of the lifetime of density fluctuations and thus in a reduction of the dominant relaxation time that we calculated. In particular, our model shows that the dynamics can be changed even at fixed density, in agreement with experiments. The main point here is that *what matters is not the average free volume (or density of the system), but its distribution*. According to the model proposed here, a broader distribution of free volume, even at fixed average density (which is obtained by heating the sample at fixed volume), results in an acceleration of the dynamics. The dynamics that

we describe here depends on the whole spectrum of density fluctuations.<sup>41</sup> The most frequent interpretation of experimental results regarding the dependence of the dynamics as a function of the two parameters  $T$  and  $\rho_{eq}$  is that the part that cannot be accounted for by the average density  $\rho_{eq}$  is entirely due to energy barriers. Our model shows that it is not true. For instance, changing the temperature at fixed density results in a change of the density fluctuations spectrum which results, within our picture, in a change of the dynamics, as we have seen in Figure 8 and the related discussion.

We hope that our results will stimulate more systematic studies of nonpolar molecular liquids, which could therefore be considered as model systems for making progress in the understanding of glass transition mechanisms. Our results suggest also that nonpolar flexible polymers, e.g., silicone polymers such as PMTS and PMPS, are also systems which could be used as model polymer systems. A more precise understanding of relaxation mechanisms in these simple systems is essential for making significant progress regarding the relaxation mechanisms in more complex systems such as polymers with temperature-dependent Kuhn length and with polar groups.

## Appendix. Evolution of the Relaxation Time $\tau_\alpha$ as a Function of Pressure

In this section, we derive eq 54 for the evolution of the relaxation time  $\tau_\alpha$  with the pressure. Let us start from an equilibrium situation at temperature  $T$  and under the pressure  $P$ . The dominant relaxation time in these conditions is given by

$$\tau_\alpha(P) = \tau_0 \exp\left(\frac{\Theta}{\tilde{\epsilon}[\tilde{\rho}_0(P); \rho_{eq}(P)]}\right) \quad (58)$$

where  $\rho_{eq}(P)$  is the mean (and equilibrium) value of the density under the applied pressure  $P$  at the considered temperature and we have defined

$$\tilde{\epsilon}[\tilde{\rho}_0; \rho] = \frac{\tilde{\rho}_0 - \rho}{\rho_0} \quad (59)$$

and where we assume that  $\tilde{\rho}_0$  is a function of pressure. Under the pressure  $P$ , the equality (51) is satisfied, which reads

$$\tau_0 \exp\left(\frac{\Theta}{\tilde{\epsilon}[\tilde{\rho}_0(P); \rho_{eq}(P)]}\right) = N_c^{2/3}(P) \tau_0 \exp\left(\frac{\Theta}{\tilde{\epsilon}[\tilde{\rho}_0(P); \rho_{eq}(P)] + (\alpha_c + \alpha_\eta)\epsilon(P)/N_c^{1/2}(P)}\right) \quad (60)$$

where  $\alpha_c$  is defined by eq 35. We have defined

$$\epsilon(P) = \frac{\rho_0 - \rho_{eq}(P)}{\rho_0} \quad (61)$$

Because of the equality (60), the evolution of  $N_c$  with the applied pressure is given by

$$N_c(P) = \frac{\Theta^2 \epsilon^2(P)}{\tilde{\epsilon}^4(P)} \frac{1}{\left(\ln\left(\frac{\Theta^2 \epsilon^2(P)}{\tilde{\epsilon}^4(P)}\right)\right)^2} \quad (62)$$

Let us suppose now that we apply a (small) increment of pressure  $\delta P$ . The dominant relaxation time as a function of temperature is then given by the WLF law at the new pressure, i.e., with a new parameter  $\tilde{\epsilon}(P + \delta P)$ :

$$\tau_\alpha(P + \delta P) = \tau_0 \exp\left(\frac{\Theta}{\tilde{\epsilon}[\tilde{\rho}_0(P + \delta P); \rho_{eq}(P + \delta P)]}\right) \quad (63)$$

According to eq 51, the dominant relaxation time at the pressure  $P + \delta P$  will also be controlled by the relaxation time of the less dense subunits. One has thus



$$\tau_0 \exp\left(\frac{\Theta}{\tilde{\epsilon}[\tilde{\rho}_0(P + \delta P); \rho_{eq}(P + \delta P)]}\right) = N_c^{2/3}(P) \tau_0 \exp\left(\frac{\Theta}{\tilde{\epsilon}[\tilde{\rho}_0(P); \rho_{eq}(P + \delta P)] + (\alpha_c + \alpha_\eta)\epsilon(P + \delta P)/N_c^{1/2}(P)}\right) \quad (64)$$

We can describe the evolution of  $\tilde{\rho}_0(P)$  as a function of pressure, i.e., regarding the pressure dependence of the WLF parameters by taking the logarithm of the eqs 60 and 64:

$$\frac{\Theta}{\tilde{\epsilon}[\tilde{\rho}_0(P); \rho_{eq}(P)]} = \frac{2}{3} \ln(N_c(P)) + \frac{\Theta}{\tilde{\epsilon}[\tilde{\rho}_0(P); \rho_{eq}(P)] + (\alpha_c + \alpha_\eta)\epsilon(P)/N_c^{1/2}(P)} \quad (65)$$

and

$$\frac{\Theta}{\tilde{\epsilon}[\tilde{\rho}_0(P + \delta P); \rho_{eq}(P + \delta P)]} = \frac{2}{3} \ln(N_c(P)) + \frac{\Theta}{\tilde{\epsilon}[\tilde{\rho}_0(P); \rho_{eq}(P + \delta P)] + (\alpha_c + \alpha_\eta)\epsilon(P + \delta P)/N_c^{1/2}(P)} \quad (66)$$

From these equations, we deduce that  $\tilde{\rho}_0(P)$  satisfies to the following differential equation

$$\frac{d}{dP} \left[ \frac{\Theta}{\tilde{\epsilon}[\tilde{\rho}_0(P); \rho_{eq}(P)]} \right] = \frac{\partial}{\partial \rho_{eq}} \left[ \frac{\Theta}{\tilde{\epsilon}[\tilde{\rho}_0(P); \rho_{eq}] + (\alpha_c + \alpha_\eta)\epsilon[\rho_{eq}]/N_c^{1/2}(P)} \right] \frac{d}{dP} [\rho_{eq}(P)] \quad (67)$$

which is exactly eq 54.

## References and Notes

- Ediger, M. D.; Angell, C. A.; Nagel, S. R. *J. Phys. Chem.* **1996**, *100*, 13200–13212.
- Review articles in: *Science* **1995**, *267*, 1924.
- Ferry, J. D. In *Viscoelastic Properties of Polymers*; John Wiley and Sons: New York, 1980.
- Rehage, G.; Oels, H. J. *High Temp.—High Pressures* **1977**, *9*, 545.
- Atake, T.; Angell, C. A. *J. Phys. Chem.* **1979**, *83*, 3218–3223.
- Patterson, G. D.; Stevens, J. R.; Carroll, P. J. *J. Chem. Phys.* **1982**, *77*, 622–624.
- Fytas, G.; Dorfmueller, Th.; Wang, C. H. *J. Phys. Chem.* **1983**, *87*, 5041–5045.
- Naoki, M.; Endou, H.; Matsumoto, K. *J. Phys. Chem.* **1987**, *91*, 4169–4174.
- Colucci, D. M.; McKenna, G. B.; Filliben, J. J.; Lee, A.; Curliss, D. B.; Bowman, K. B.; Russell, J. D. *J. Polym. Sci., Part B: Polym. Phys.* **1997**, *35*, 1561–1573.
- McKenna, G. B.; Vangel, M. G.; Rukhin, A. L.; Leigh, S. D.; Lotz, B.; Straupe, C. *Polymer* **1999**, *40*, 5183–5205.
- Paluch, M.; Hensel-Bielowska, S.; Ziolo, J. *J. Chem. Phys.* **1999**, *110*, 10978–10981.
- Huang, D.; Colucci, D. M.; McKenna, G. B. *J. Chem. Phys.* **2002**, *116*, 3925–3934.
- Paluch, M.; Casalini, R.; Best, A.; Patkowski, A. *J. Chem. Phys.* **2002**, *117*, 7624–7630.
- Paluch, M.; Casalini, R.; Roland, C. M. *Phys. Rev. B* **2002**, *66*, 1–3.
- Paluch, M.; Pawlus, S.; Roland, C. M. *Macromolecules* **2002**, *35*, 7338–7342.
- Casalini, R.; Paluch, M.; Roland, C. M. *Phys. Rev. E* **2003**, *67*, 1–6.
- McKinney, J. K.; Simha, R. *Macromolecules* **1974**, *7*, 894–901.
- Roland, C. M.; Casalini, R. *Macromolecules* **2003**, *36*, 1361–1367.
- Paluch, M.; Casalini, R.; Patkowski, A.; Pakula, T.; Roland, C. M. *Phys. Rev. E* **2003**, *68*, 1–5.
- Paluch, M.; Roland, C. M.; Casalini, R.; Meier, G.; Patkowski, A. *J. Chem. Phys.* **2003**, *118*, 4578–4582.
- Barbieri, A.; Gorini, G.; Leporini, D. *Phys. Rev. E* **2004**, *69*, 1–5.
- Casalini, R.; Paluch, M.; Roland, C. M. *J. Chem. Phys.* **2003**, *118*, 5701–5703.
- Wang, B.; Wang, Z. F.; Zhang, M.; Liu, W. H.; Wang, S. J. *Macromolecules* **2002**, *35*, 3993–3996.
- Paluch, M.; Pawlus, S.; Roland, C. M. *Macromolecules* **2002**, *35*, 7338–7342.
- Kahle, S.; Gapinski, J.; Hinze, G.; Patkowski, A.; Meier, G. *J. Chem. Phys.* **2005**, *122*, 1–10.
- Pawlus, S.; Bartos, J.; Sausa, O.; Kristiak, J.; Paluch, M. *J. Chem. Phys.* **2006**, *124*, 1–5.
- Ferrer, M. L.; Lawrence, C.; Demirjian, B. G.; Kivelson, D.; Alba-Simionesco, C.; Tarjus, G. *J. Chem. Phys.* **1998**, *109*, 8010–8015.
- Alba-Simionesco, C.; Kivelson, D.; Tarjus, G. *J. Chem. Phys.* **2002**, *116*, 5033–5038.
- Roland, C. M.; Paluch, M.; Pakula, T.; Casalini, R. *Philos. Mag.* **2004**, *84*, 1573–1581.
- Roland, C. M.; Bair, S.; Casalini, R. *J. Chem. Phys.* **2006**, *125*, 1–8.
- Schmidt-Rohr, K.; Spiess, H. W. *Phys. Rev. Lett.* **1991**, *66*, 3020–3023.
- Tracht, U.; Wilhelm, M.; Heuer, A.; Feng, H.; Schmidt-Rohr, K.; Spiess, H. W. *Phys. Rev. Lett.* **1998**, *81*, 2727–2730.
- Cicerone, M. T.; Blackburn, F. R.; Ediger, M. D. *Macromolecules* **1995**, *28*, 8224–8232.
- Thurau, C. T.; Ediger, M. D. *J. Chem. Phys.* **2003**, *118*, 1996–2004.
- Tolle, A.; Schöber, H.; Wuttke, J.; Randl, O. G.; Fujara, F. *Phys. Rev. Lett.* **1998**, *80*, 2374–2377.
- Hall, D. B.; Dhinojwala, A.; Torkelson, J. M. *Phys. Rev. Lett.* **1997**, *79*, 103–106.
- Richert, R. *J. Chem. Phys.* **2000**, *113*, 8404–8429.
- Long, D.; Lequeux, F. *Eur. Phys. J. E* **2001**, *4*, 371–387.
- Merabia, S.; Long, D. *Eur. Phys. J. E* **2002**, *9*, 195–206.
- Merabia, S.; Sotta, P.; Long, D. *Eur. Phys. J. E* **2004**, *15*, 189–210.
- Merabia, S.; Long, D. *J. Chem. Phys.* **2006**, *125*, 234901–1–234901–18.
- Dzero, M.; Schmalian, J.; Wolynes, P. G. *Phys. Rev. B* **2005**, *72*, 100201(R)–1100201(R)–4.
- Tarjus, G.; Kivelson, D. In *Jamming and Rheology: Constrained Dynamics on Microscopic and Macroscopic Scales*; Scales, S., Edwards, A., Liu, S., Nagel, Eds.; Taylor and Francis: Philadelphia, 2001.
- Donati, C.; Douglas, J. F.; Kob, W.; Plimpton, S. J.; Poole, P. H.; Glotzer, S. C. *Phys. Rev. Lett.* **1998**, *80*, 2338–2341.
- Chandler, D.; Garrahan, J. P.; Jack, R. L.; Maibaum, L.; Pan, A. C. *Phys. Rev. E* **2006**, *74*, 051501–1–051501–9.
- Saltzman, E. J.; Schweizer, K. S. *J. Chem. Phys.* **2004**, *121*, 2001–2009.
- Zhang, S.; Painter, P. C.; Runt, J. *Macromolecules* **2002**, *35*, 8478–8487.
- Kovacs, A. J. *J. Polym. Sci.* **1958**, *30*, 131–147.
- Kovacs, A. J.; Aklonis, J. J.; Hutchinson, J. M.; Ramos, A. R. *J. Polym. Sci., Polym. Phys. Ed.* **1979**, *17*, 1097–1162.
- Israelachvili, J. N. In *Intermolecular and Surface Forces*; Academic Press: London, 1992.
- Press, W. H.; Teukolsky, S. A.; Vetterling, W. T.; Flannery, B. P. In *Numerical Recipes in Fortran*; Cambridge University Press: New York, 1992.
- McKinney, J. E.; Goldstein, M. *J. Res. Natl. Bur. Stand.* **1974**, *78A*, 331–353.
- Naoki, M.; Koeda, S. *J. Phys. Chem.* **1989**, *93*, 948–955.
- Mark, J. E. In *Physical Properties of Polymers Handbook*; American Institute of Physics: New York, 1996.
- Plazek, D. *J. Polym. Sci.* **1980**, *12*, 43–53.
- Plazek, D. *J. Polym. Sci., Polym. Phys. Ed.* **1982**, *20*, 729–742.
- Dreyfus, C.; Aouadi, A.; Gapinski, J.; Matos-Lopes, M.; Steffen, W.; Patkowski, A.; Pick, R. M. *Phys. Rev. E* **2003**, *68*, 011204–1–011204–11.
- Roland, C. M.; McGrath, K. J.; Casalini, R. *J. Non-Cryst. Solids* **2006**, *352*, 4910–4914.
- Floudas, G.; Mpoukouvalas, K.; Papadopoulos, P. *J. Chem. Phys.* **2006**, *124*, 1–5.
- Casalini, R.; Roland, C. M. *Phys. Rev. E* **2005**, *72*, 031503–1–031503–4.
- Reiser, A.; Kasper, G.; Hunklinger, S. *Phys. Rev. B* **2005**, *72*, 094204–1–094204–7.
- Ngai, K. L.; Casalini, R.; Roland, C. M. *Macromolecules* **2005**, *38*, 4363–4370.
- Roland, C. M.; Casalini, R. *Macromolecules* **2005**, *38*, 8729–8733.
- Casalini, R.; Mohanty, U.; Roland, C. M. *J. Chem. Phys.* **2006**, *125*, 014505–1–014505–9.

MA702524J